Integrated Photonic Resonant Modulator-Based Equalization and Optimization for DWDM

Asher Novick,[1,*,†] Maarten Hattink,[1,†] Anthony Rizzo,[1] Yuyang Wang,[1] Vignesh Gopal,[1] Songli Wang,[1] Robert Parsons,[1] and Keren Bergman[1]

[1]*Department of Electrical Engineering, Columbia University, New York, NY, 10027, USA*
[†]*Now at Xscape Photonics*
[*]*asher.novick@columbia.edu*

Abstract: We perform multi-wavelength signal equalization and optimization in a DWDM SiPh link by adjusting the operating regime of integrated resonant modulators. An effective increase in the optical link's dynamic range of >3 dB is measured. © 2024 The Author(s)

1. Introduction

The next generation of optical interconnects for data center (DC) and high-performance computing (HPC) applications require unprecedented integrated optical bandwidth density and energy efficiency metrics. Recent advances in optical frequency comb sources and novel integrated photonic link architectures are meeting these metrics via dense wavelength-division multiplexing (DWDM) [1]. In such systems, the maximum total aggregated per-fiber link bandwidth is the per-channel signal bandwidth multiplied by the number of distinct carrier wavelength channels used, which is limited by the optical channel spacing and the total usable bandwidth in the optical domain. For DC and HPC applications where maintaining the optical link budget is key, spectral non-uniformity throughout the interconnect can become an obstacle towards full bandwidth utilization, requiring complex and power-hungry receiver designs with large dynamic range [2].

Integrated resonant modulators have matured as a commercially viable technology, capable of supporting broadband DWDM applications up to per channel data rates beyond 25 Gbps/λ [3]. These modulators are attractive due to their compact footprint, high modulation efficiency compatible with standard complementary metal-oxide-semiconductor (CMOS) peak-to-peak drive voltages (V_{pp}), and inherent wavelength selectivity. Fundamental to the operation of resonant modulators is the trade-off between insertion loss (IL) and signal extinction ratio (ER) for a given V_{pp}, determined by selection of the de-tuning wavelength ($\Delta\lambda$) between the optical carrier and the modulator resonance [4]. Typically, the ideal operational $\Delta\lambda$ is defined to minimize the transmission power penalty (PP_{total}) for each individual channel, disregarding the wavelength-dependent signal penalties of the interconnects.

Here, we propose utilizing the inherent relationship between a resonant modulator's IL and ER to perform dynamic and adaptable broadband DWDM equalization and signal optimization. By operating modulators at different values of $\Delta\lambda$, wavelength channels corresponding to lower power penalties can be operated with larger modulator IL and ER, flattening the spectrum and improving average signal ER across the link and reducing crosstalk due to the relative power between victim and aggressor channels at the receiver. Through this technique, we experimentally demonstrate >3 dB of effective increase in receiver dynamic range by dynamically tuning the resonant modulator's $\Delta\lambda$ and V_{pp}.

2. Measurement-based Equalization Model

For on-off keying non-return to zero modulation (OOK-NRZ), the IL and ER are defined relative to the modulator optical power input (P_{in}) and power output of a "1" (P_1) and a "0" (P_0). In dB units, $IL = -10\log_{10}(P_1/P_{\mathrm{in}})$ and $ER = 10\log_{10}(P_1/P_0)$, while the corresponding linear terms are simply $l = P_1/P_{\mathrm{in}}$ and $r = P_1/P_0$. PP_{total} for OOK-NRZ modulation, inversely related to optical modulation amplitude (OMA), can be calculated as $PP_{\mathrm{total}} = IL + 10\log_{10}\left(\frac{2r}{r+1}\right) + 10\log_{10}\left(\frac{r+1}{r-1}\right)$ [1]. We define a normalized OMA (OMA/P_{in}),

$$OMA/P_{\mathrm{in}} = (P_1 - P_0)/P_{\mathrm{in}} = l\,(1 - 1/r) \tag{1}$$

In the case of depletion-mode resonant modulators, IL and ER as functions of $\Delta\lambda$ and V_{pp} are derived from the DC depletion response measurements, illustrated in Fig. 1. As noted in prior works, resonant modulators suffer from self heating effects under normal operating conditions, resulting in stable performance only when $\Delta\lambda <$ 0 nm. For a link comprised of a single carrier wavelength, maximizing the receiver's photodiode peak-to-peak

photocurrent (I_{pp}) results in the highest quality signal. In the case of Fig. 1c, this corresponds to $\Delta\lambda \approx -0.05$ nm for $V_{pp} = 1.5$ V.

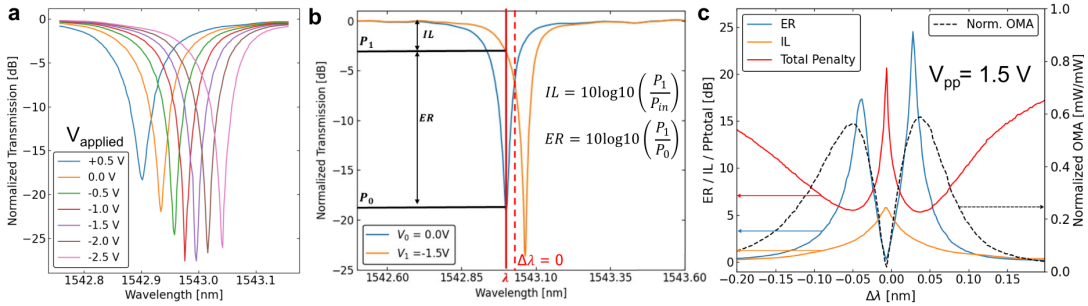

Fig. 1. **a)** Measured depletion response of an on-chip microdisk modulator. **b)** IL and ER at each wavelength is calculated based on the relative transmission of the spectra at V_0 and V_1 states. $\Delta\lambda = 0$ halfway between resonance states. **c)** ER and IL curves for $V_{pp} = 1.5$ V. PP_{total} is plotted on the same axes, while OMA/P_{in} is plotted on the right y-axis. Minimum PP_{total} corresponds to maximum OMA/P_{in}.

Instead, we consider a DWDM link consisting of many independently modulated λs multiplexed along a single channel. Due to a combination of factors, such as a non-flat multi-λ source, wavelength-dependent optical loss (and/or gain), or even the receiver photodiode's responsivity (in A/W), spectral non-uniformity is inevitable [1]. Eq. (2) defines an operational space based on the expected I_{pp} for each carrier λ in a resonant modulator–driven DWDM system.

$$I_{pp}(\lambda, \Delta\lambda, V_{pp}) = P_{in}(\lambda) \times \frac{OMA}{P_{in}}(\Delta\lambda, V_{pp}) \times 10^{IL_{link}(\lambda)/10} \times R_{PD}(\lambda) \tag{2}$$

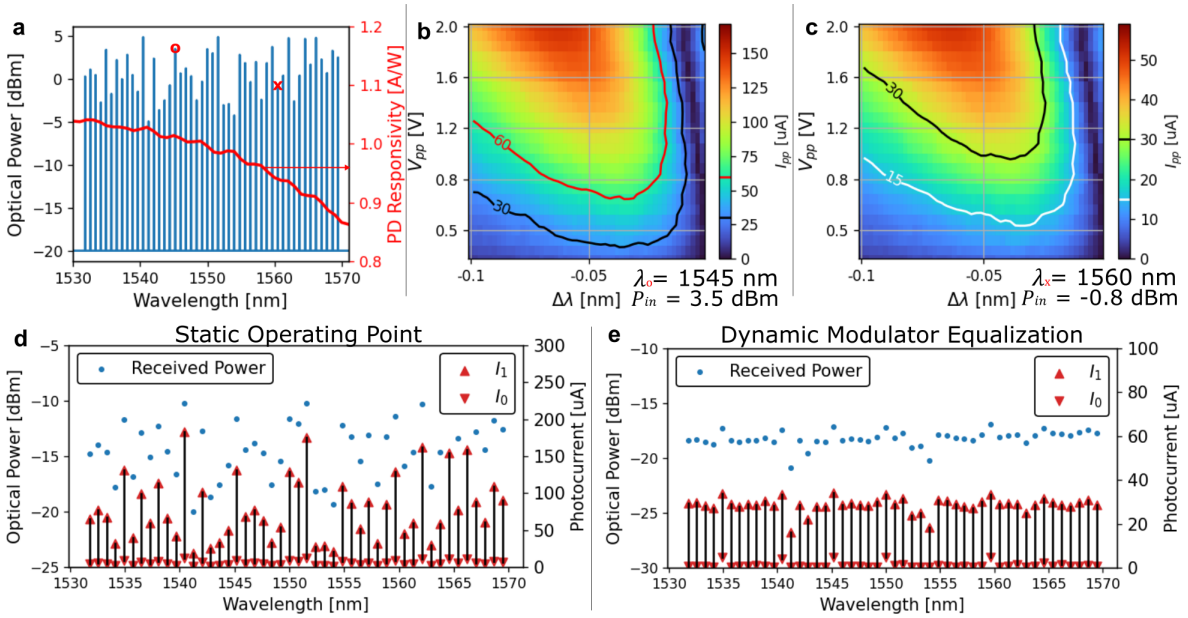

Fig. 2. **a)** Modeled DWDM source with power per λ covering 10 dB dynamic range and measured integrated photodiode responsivity at -1 V reverse bias. Assuming $IL_{link} = 10$ dB, **b)** expected $I_{pp}(\lambda_o = 1545\,\text{nm}, \Delta\lambda, V_{pp})$ and **c)** expected $I_{pp}(\lambda_x = 1560\,\text{nm}, \Delta\lambda, V_{pp})$. Received optical power and I_{pp} operating each channel **d)** statically at the largest OMA for $V_{pp} = 1.5$ V and **e)** dynamically for $0.5\,\text{V} \leqslant V_{pp} \leqslant 1.5\,\text{V}$ and $-0.1\,\text{nm} \leqslant \Delta\lambda \leqslant 0\,\text{nm}$ to maximizing ER and I_{pp}, with minimum $I_{pp} = 15\,\mu\text{A}$ and a 3 dB dynamic range limit.

Fig. 2a shows a synthesized DWDM source with 10 dB difference in power between minimum and maximum carrier wavelengths. Plotted on the secondary y-axis is a measured germanium photodiode integrated on a silicon

chip showing the $R_{\mathrm{PD}}(\lambda)$ profile. With this DWDM source and photodiode, assuming a spectrally uniform $IL_{\mathrm{link}} = 10\,\mathrm{dB}$ and using the measured disk modulator from Fig. 1, Fig. 2b-c show the expected $I_{\mathrm{pp}}(\Delta\lambda, V_{\mathrm{pp}})$ at the receiver for high and low power λs, respectively. Fig. 2d shows the received optical power and photocurrents of each DWDM channel, for a fixed $V_{\mathrm{pp}} = 1.5\,\mathrm{V}$, when $\Delta\lambda$ is chosen for maximum OMA, showing approximately the same dynamic range as the DWDM source. In contrast, Fig. 2e illustrates our proposed model of dynamically tuning both V_{pp} and $\Delta\lambda$ to achieve an equalized signal at the receiver. In addition to equalizing the signals' dynamic range across the spectrum, the model results in a larger average ER (15.2 dB vs 11.6 dB) and a lower average modulator V_{pp} (0.9 V vs 1.5 V), improving signal quality and saving power ($E_b = \frac{1}{4}CV_{\mathrm{pp}}^2\,[\frac{\mathrm{J}}{\mathrm{bit}}]$) [1].

3. Field-Programmable Gate Array (FPGA)–Driven WDM Transmission Demonstration

The proposed technique is demonstrated on multiple λs with a FPGA-driven packaged SiP microdisk modulator-based WDM transmitter board. The FPGA generates a pair of uncorrelated pseudo-random bit sequences (PRBS) of $2^{15}-1$ bits length at 5 and 10 Gbps, with a range of $0.2\,\mathrm{V} \leqslant V_{\mathrm{pp}} \leqslant 0.4\,\mathrm{V}$. $\Delta\lambda$ was tuned via an integrated heater dissipating power (P_{th}) with $\partial\Delta\lambda \propto \partial P_{\mathrm{th}}$. The microdisk modulators have a resonance extinction ratio $\approx 10\,\mathrm{dB}$ and modulation efficiency $\approx 8\,\mathrm{GHz/V}$ [3].

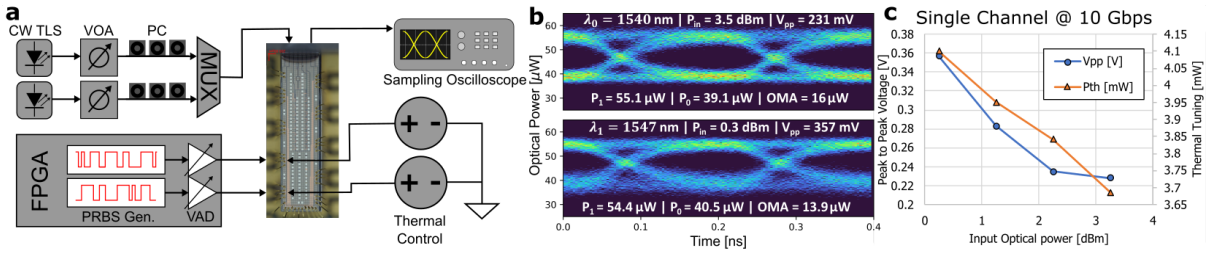

Fig. 3. **a)** Diagram of WDM experiment. Two wavelengths, at different power levels, are modulated by cascaded micro disk modulators (micrograph shows packaged PIC). The modulators are driven with PRBS sequences by a FPGA and their $\Delta\lambda$ operating points are set using lab power supplies. **b)** Equalized 5 Gbps eye diagrams for $\lambda_0 = 1540\,\mathrm{nm}$, $P_{\mathrm{in}} = 3.25\,\mathrm{dBm}$, and $V_{\mathrm{pp}} = 231\,\mathrm{mV}$ and $\lambda_1 = 1547\,\mathrm{nm}$, $P_{\mathrm{in}} = 0.25\,\mathrm{dBm}$, and $V_{\mathrm{pp}} = 357\,\mathrm{mV}$. **c)** Measured relationship between V_{pp}, P_{th}, and P_{in} to maintain constant OMA and P_1 for λ_0 modulated at 10 Gbps.

4. Conclusion

We describe and demonstrate the efficacy of on-chip resonant SiP modulator-based DWDM equalization and optimization over a broad optical bandwidth. In principle, this technique is agnostic to the specific implementation of resonant modulator and can be adaptively tuned to compensate for an established link's particular sources of spectral non-uniformity, including time varying factors.This method significantly differs from prior demonstrations of spectral equalization, such as gain flattening filters for EDFAs, in that the implementation requires no additional components in the optical link. In addition to reducing the average energy consumed by modulation, this technique reduces inter-channel crosstalk between adjacent spectral channels increasing the overall link budget. The upper limit on effective dynamic range improvement is determined primarily on the range of V_{pp} and resonator extinction ratio. With common CMOS drive voltages it would be practical to realize $\geqslant 10\,\mathrm{dB}$ increase in dynamic range.

References

1. A. Rizzo, S. Daudlin, A. Novick *et al.*, "Petabit-scale silicon photonic interconnects with integrated kerr frequency combs," IEEE J. Sel. Top. Quantum Electron. **29**, 1–20 (2022).
2. A. A. Afzalian and D. Flandre, "Design of multi gb/s monolithically integrated photodiodes and multi-stage transimpedance amplifiers in thin-film soi cmos technology," in *Photodiodes,* I. Yun, ed. (IntechOpen, Rijeka, 2012), chap. 11.
3. N. M. Fahrenkopf *et al.*, "The aim photonics mpw: A highly accessible cutting edge technology for rapid prototyping of photonic integrated circuits," IEEE J. Sel. Top. Quantum Electron. **25**, 1–6 (2019).
4. M. de Cea *et al.*, "Power handling of silicon microring modulators," Opt. Express **27**, 24274–24285 (2019).

Acknowledgements: This work was supported in part by the U.S. Defense Advanced Research Projects Agency under PIPES Grant HR00111920014 and in part by the U.S. Advanced Research Projects Agency–Energy under ENLITENED Grant DE-AR000843.